Desalination and Water Treatment
www.deswater.com

doi: 10.5004/dwt.2022.28537

262 (2022) 248–255
June

Facile synthesis of nanostructured ZnCuBi-NO_3/SO_4 layered double hydroxides for photocatalytic degradation of methylene blue

Abdul Nabi Jakhrani[a], Aydan Elçi[b], Ali Nawaz Siyal[a,*], Adnan Ahmed[c], Baddar Ul Ddin Jamali[a], Abdul Ghani Jakhrani[d], Naeem Piyaro Butt[a], Saima Qayoom Memon[a]

[a]*Institute of Chemistry, University of Sindh, Jamshoro 76080, Pakistan, Tel. +92 22 921311, Ext. 2004; emails: alinsiyal@usindh.edu.pk/alinawazsiyal@yahoo.com (A.N. Siyal), abdulnabi4753@gmail.com (A.N. Jakhrani), badarddin2@hotmail.com (B. Ul Ddin Jamali), piyaronaeem@gmail.com (N.P. Butt), msaima77@gmail.com/saimaqmemon@usindh.edu.pk (S.Q. Memon)*
[b]*Department of Chemistry, University of Ege, Bornova 35040, Izmir, Turkey, Tel. +90-2323399091; email: aydan.elci@ege.edu.tr (A. Elçi)*
[c]*Center for Environmental Science, University of Sindh, Jamshoro 76080, Pakistan, Tel. +92 333 2891399; email: adnan.jaat@gmail.com (A. Ahmed)*
[d]*Department of Environmental Engineering, Quaid-E-Awam University of Engineering, Science and Technology, Nawab Shah 67480, Pakistan, Tel. +92-3003102383; email: ghanibaloch168@gmail.com (A.G. Jakhrani)*

Received 23 November 2021; Accepted 26 April 2022

ABSTRACT

In this study, nanostructured ZnCuBi-NO_3/SO_4 layered double hydroxides (LDH) was developed followed by a co-precipitation approach using precursors such as $ZnSO_4{\cdot}7H_2O$, $CuSO_4{\cdot}5H_2O$ and $Bi(NO_3)_3{\cdot}5H_2O$, and well characterized by Fourier-transform infrared spectroscopy, X-ray diffraction, energy-dispersive X-ray spectroscopy-scanning electron microscopy, and thermogravimetric analysis techniques. Using absorbance data, Tauc plot was plotted and band gap energy of ZnCuBi LDH was calculated and found to be 1.73 eV. The material was applied as an efficient photocatalyst for degradation of methylene blue (MB) under visible light of a 100 W Tungsten lamp at optimum factors such as concentration of MB 10 mg L^{-1}, pH 8.0, catalyst dosage 10 mg, and shaking time of 30 min at room temperature. The degradation efficiency of the material was calculated and found to be ≥95.5% with RSD ≤4%. The method worked well on the synthetic solutions of MB, prepared in tap water, wastewater, and seawater of different concentrations.

Keywords: Layered double hydroxides; Photocatalysis; Methylene blue; Wastewater; Degradation

1. Introduction

An undesirable change in the biological, physical, chemical characteristics of water, land, and air, is said to be pollution. The pollutants may be inorganic such as fertilizers, mineral acids, cyanides, organometallic complexes, heavy metal ions, metalloids, etc. [1–4], and organic such as paints, pigments, and dyes including methylene blue, methylene orange, and methylene red, etc. [5,6]. The direct discharge of dyes-contaminated wastewater causes a serious threat to aquatic bodies. Treatment of organic contaminated wastewater is strongly advised prior to release into aqueous bodies [7]. A variety of treatment methods, including ion exchange, membrane filtration,

* Corresponding author.

adsorption, and photocatalytic degradation are documented [8]. Photocatalytic degradation is more attractive because of the eco-friendly, cost-effective, and high degradation efficiency of the material [9]. Various semiconductor metal oxides such as ZnO [10], TiO_2 [11], Fe_2O_3 [12], CuO [13], CdO [14], SnO_2 [15], WO_3 [16], Bi_2O_3 [17], Ag_2CO_3 [18], Ag_3PO_4 [19] and LDHs such as ZnAl, MgAl [20], CdS/CoAl [21], NiAl [22], MgAl [23], MgFeTi [24] and MgZnAlFe [25] have been applied as photocatalysts for degradation of organic dyes. LDHs are anionic clays, consisting of positively charged metal hydroxide sheets with intercalated anions (OH^-, NO_3^- and SO_4^{2-}, etc.) and water molecules [26,27]. Generally, LDH is represented by the formula $[M^{2+}_{1-x}M^{3+}_x(OH)_2]^{x+}(A^{n-}_{x/n})\cdot yH_2O$, where M^{2+} is divalent and M^{3+} is trivalent metal ions, x is equal to molar ratio of $M^{3+}/(M^{2+} + M^{3+})$, A^{n-} is n valent anion(s), and y is number of intercalated water molecules [28,29]. This study focused on the synthesis of ZnCuBi-NO_3/SO_4 LDH for the degradation of methylene blue (MB).

2. Material and method

2.1. Chemical and equipment

Chemicals and equipment are enlisted in Tables 1 and 2, respectively. For solutions preparation, double distilled water was used throughout the research.

2.2. Synthesis of ZnCuBi-NO_3/SO_4 LDH

The ZnCuBi LDH was synthesized followed by the co-precipitation method. Experimentally, four aqueous solutions were prepared such as *A*: 250 mL of 2.0 mol L^{-1} NaOH, *B*: 250 mL of 0.025 mol L^{-1} $ZnSO_4\cdot 7H_2O$, *C*: 250 mL of 0.025 mol L^{-1} $CuSO_4\cdot 5H_2O$, and *D*: 250 mL of 0.025 mol L^{-1} $Bi(NO_3)_3\cdot 5H_2O$. *D* contained 20 mL of concentrated HNO_3 for a reason to solubilize bismuth salt. All these four solutions were poured into burettes separately and added dropwise into a beaker containing 50 mL of water, with continuous stirring at 55°C and maintaining pH 9 ± 0.5 throughout the reaction. The precipitated ZnCuBi-NO_3/SO_4 LDH was filtered, washed with water until became neutral, finally washed with acetone, and oven-dried at 100°C for 24 h. The synthesized LDH was stored in a clean tube for further experiments.

2.3. Photocatalysis experiment

Experimentally, 10 mg of ZnCuBi-NO_3/SO_4 LDH was taken into a 25 mL bottle, containing 10 mL of 10 mg L^{-1} MB of pH 8.0 and stirred in dark for 30 min for achieving adsorption–desorption equilibrium. Thereafter, photocatalysis was triggered by exposing the mixture under visible light of a 100 W Tungsten lamp, and stirred at 25°C for 30 min. The mixture was centrifuged at 10,000 rpm and subjected to UV/Visible spectrophotometer at λ_{max} of 664 nm for quantitative study of MB. The degradation efficiency was calculated by Eq. (1) and achieved ≥95.50% with RSD ≤4.0%. The degradation reaction setup and mechanism are depicted in Fig. 1.

$$\text{Degradation efficiency}\,(\%) = \left(\frac{C_i - C_f}{C_i}\right)\times 100 \quad (1)$$

where C_i and C_f are the final concentrations of MB before and after degradation, respectively.

3. Results and discussion

3.1. Characterization

3.1.1. Fourier-transform infrared spectroscopy

Fig. 2 depicts the Fourier-transform infrared spectroscopy (FT-IR) spectrum of ZnCuBi-NO_3/SO_4 LDH. The characteristics stretching vibration at 3,413 cm^{-1} corresponds to the O–H bond of the hydroxyl group of LDH and intercalated H_2O molecules [30], peaks at 1,627 cm^{-1} is assigned to OH bond of intercalated water molecules [31,32], a strong peak at 1,356 cm^{-1} is assigned to

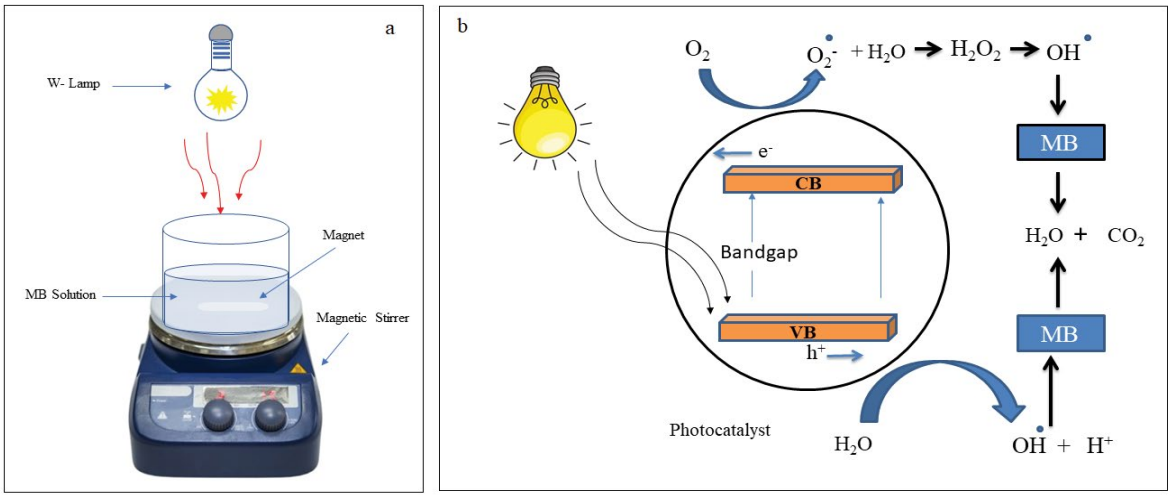

Fig. 1. Home-made degradation set-up (a) and mechanism of photocatalysis for the degradation of MB (b).

Table 1
Chemicals used throughout the research

Particulars	Brand/Company	Purposes
$CuSO_4 \cdot 5H_2O$ (98.0%), $Bi(NO_3)_3 \cdot 5H_2O$ (98.0%), $ZnSO_4 \cdot 7H_2O$ (99.0%)	Sigma-Aldrich, China	Material synthesis
CH_3COOH (≥99%), CH_3COONa (≥99%) NaOH (99.0%), HCl (≥37.0%), NH_4OH (25%–28%), NH_4Cl (≥99.5%), H_3PO_4 (87.32%), NaH_2PO_4 (99.0%)	Sigma-Aldrich, China	Buffer solutions preparation
Methylene blue	Merck, USA	Degradation study

Table 2
Equipment used throughout the research

Particulars	Brand/Company	Purposes
Nicolet iS10 FT-IR spectrometer	Thermo Scientific, UK	Characterization
D8 ADVANCE X-ray diffractometer, X-ray: Cu-Kα (λ = 1.54056 Å)	Bruker, Germany	Powder XRD analysis
Scanning electron microscope	JSM-6490LV, JEOL, Japan	SEM analysis
XFlash detector 4010 133 eV, X-ray: Cu-Kα (λ = 1.5406 Å)	Bruker, Germany	EDX analysis
Shaker	Model No.1-4000, Germany	Shaking
pH meter	InoLab pH 720, Germany	pH measurement

N=O bond of interacted nitrate ions [30], sharp peak at 1,112 cm^{-1} corresponds to S=O bond of intercalated sulfate ions [33], and weak peak at 849 cm^{-1} demonstrates the metal-oxygen linkages of ZnCuBi-NO_3/SO_4 LDH [30].

3.1.2. X-ray diffraction

Fig. 3 depicts the powder X-ray diffraction (XRD) pattern of ZnCuBi-NO_3/SO_4 LDH. Peaks at 2θ values of 11.5° and 27.2° are assigned to 003 and 006 planes (hkl) of ZnCuBi-NO_3/SO_4 LDH crystal system, respectively, revealing the formation of hydrotalcite-like structure of LDH [34]. Using Bragg's law, the d spacing of 003 and 006 planes were calculated and found to be 0.77 and 0.33 nm, respectively. The material contained traces of metal oxides phases which were formed by oxidation of metal ions during the synthesis process.

3.1.3. Energy-dispersive X-ray spectroscopy-scanning electron microscopy

The elemental content in ZnCuBi-NO_3/SO_4 LDH was tested by energy-dispersive X-ray spectroscopy (EDX) analysis (Fig. 4). The LDH contains 23.32%, 0.13%, 8.13%, 8.04%, 18.58%, and 30.15% of O, S, N, Zn, Cu, and Bi, respectively, indicated the presence of O, S, N, Zn, Cu, and Bi in the synthesized LDH, which revealed the formation of ZnCuBi-NO_3/SO_4 LDH. Scanning electron microscopy (SEM) image of ZnCuBi-NO_3/SO_4 LDH at different resolutions (Fig. 5) revealed that the synthesized material was aggregated to micro-sized.

3.1.4. Thermogravimetric analysis

The thermogravimetric analysis (TGA) depicts the thermal stability of synthesized LDH. Thermogram (Fig. 6) demonstrates the fragmentation of ZnCuBi-NO_3/SO_4 LDH into three steps at different temperatures. The first step at 260°C–370°C demonstrates the loss of nitrate ions, the second step at 530°C–690°C assigns the loss of intercalated sulfate ions and the third step at 600°C–700°C revealed the degradation of metal hydroxides [35].

3.1.5. Optical study of ZnCuBi-NO_3/SO_4 LDH

UV-Visible absorption spectrum (Fig. 7) of an aqueous suspension solution of ZnCuBi-NO_3/SO_4 LDH was recorded in the region of 300–800 nm. Using absorption data, the Tauc plot was plotted as $(hv)^2$(eV cm^{-1}) vs. energy (eV), and direct band gap energy of ZnCuBi-NO_3/SO_4 LDH was calculated and found to be 1.73 eV [36].

3.2. Optimization of variables

3.2.1. pH

Influence of pH on the efficiency of ZnCuBi-NO_3/SO_4 LDH for degradation of MB was examined. Experimentally, 10 mL of 10 mg L^{-1} MB was taken into a 25 mL bottle containing 10 mg of ZnCuBi LDH. The mixture was irradiated with visible light of a 100 W Tungsten lamp, and stirred at 25°C for 30 min. The mixture was centrifuged and subjected to UV/visible spectrophotometer at λ_{max} of 664 nm for quantification. The degradation efficiency (%) was decreased at pH 4–5 and increased with further increasing of pH 5–8 as depicted in Fig. 8. Therefore, pH 8 was chosen as the working pH for further experiments.

3.2.2. Concentration

Effect of the concentration of MB solution in the range of 2.5–20 mg L^{-1} on degradation efficiency was examined. In a typical procedure, 10 mL of 2.5–20 mg L^{-1} MB of pH 8.0 was taken into a 25 mL bottle containing 10 mg of

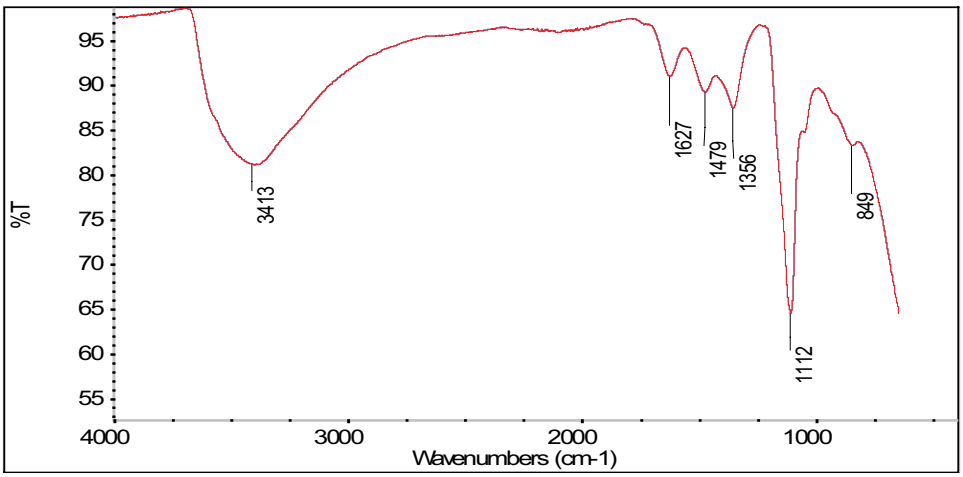

Fig. 2. FT-IR spectrum of ZnCuBi-NO_3/SO_4 LDH.

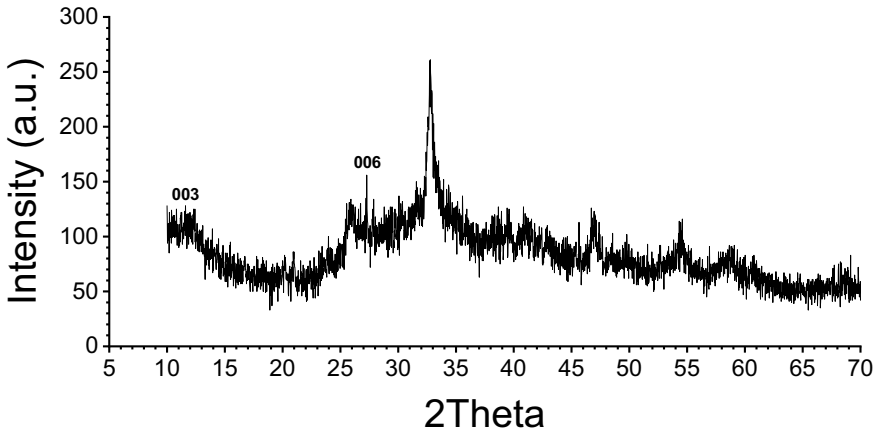

Fig. 3. Powder XRD pattern of ZnCuBi-NO_3/SO_4 LDH.

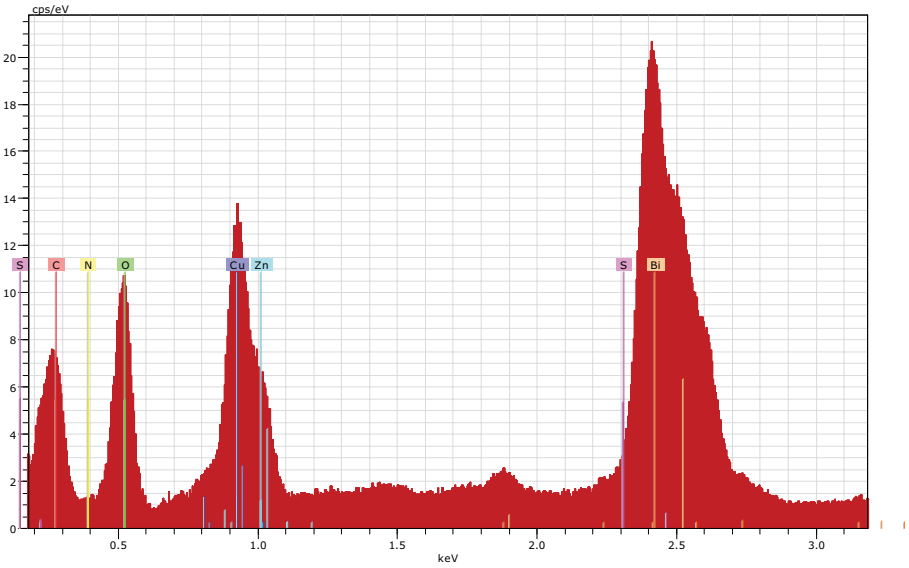

Fig. 4. EDX spectrum of ZnCuBi-NO_3/SO_4 LDH.

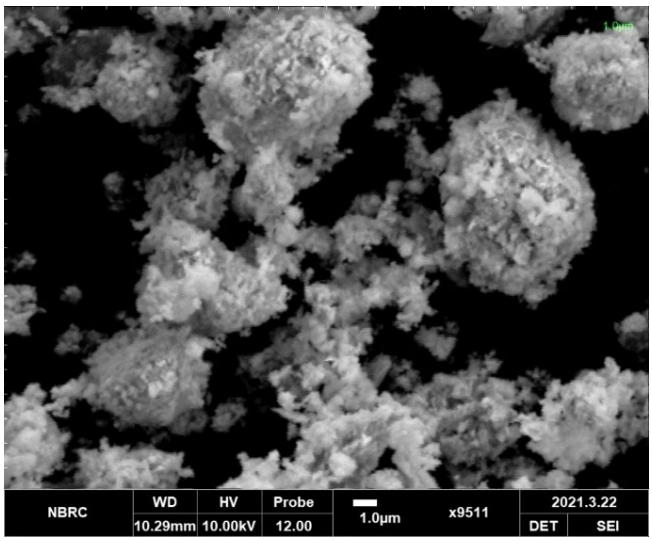

Fig. 5. SEM image of nanostructured ZnCuBi-NO_3/SO_4 LDH.

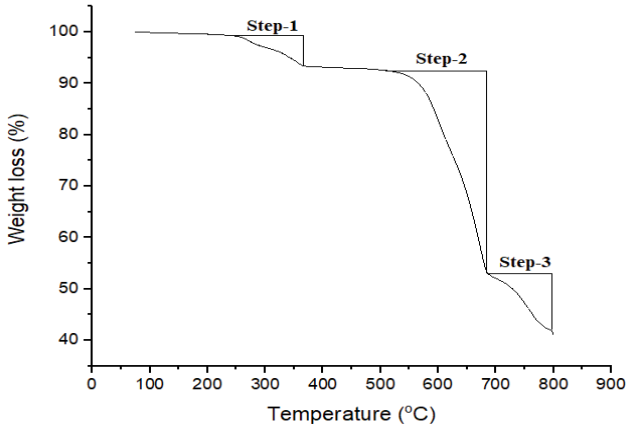

Fig. 6. Thermogram of ZnCuBi-NO_3/SO_4 LDH.

ZnCuBi-NO_3/SO_4 LDH. The mixture was exposed in visible light of a 100 W Tungsten lamp, and stirred at 25°C for 30 min. The mixture was centrifuged and subjected to UV/Visible spectrophotometer at λ = 664 nm for quantification. The degradation efficiency (%) was decreased with increasing concentration as depicted in Fig. 9. Therefore, 10 mg L^{-1} was chosen as the optimum concentration of MB for further experiments.

3.2.3. Catalyst dosage

Photocatalyst dosage is an important factor in the degradation process, so the effect of catalyst dosage was examined. In a typical procedure, 10–60 mg of doses of the LDH material were tested for degradation of 10 mL of 10 mg L^{-1} MB of pH 8. The mixture was exposed in visible light to a 100 W Tungsten lamp. Thereafter, the mixture was centrifuged and subjected to UV/Visible spectrophotometer at λ_{max} of 664 nm for quantification. The degradation efficiency was enhanced with increasing of the dose 10–20 mg and slightly changed with further increasing of the dose

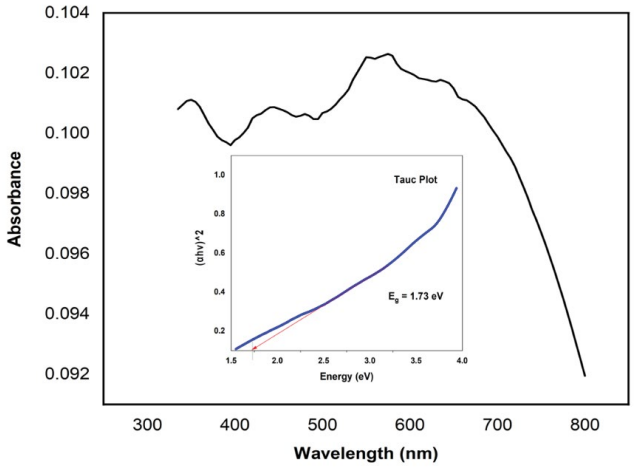

Fig. 7. Absorbance spectrum of the ZnCuBi-NO_3/SO_4 LDH and Tauc plot.

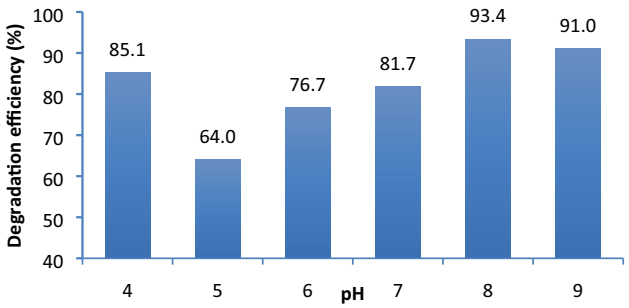

Fig. 8. Effect of pH on degradation efficiency (%) of the LDH for MB.

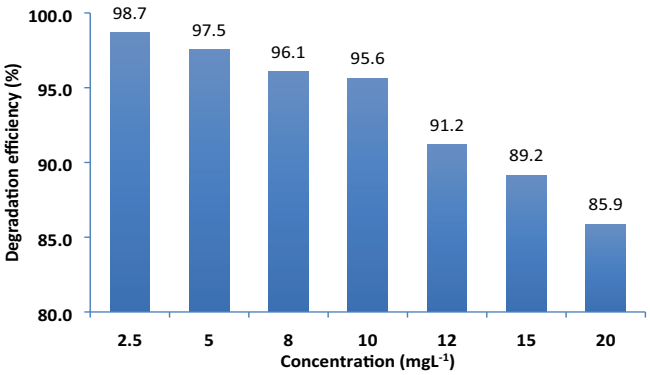

Fig. 9. Effect of concentration of MB on degradation efficiency (%) of the LDH.

20–60 mg as depicted in Fig. 10. Therefore, 10 mg was taken as the optimum catalyst dose for further experiments.

3.2.4. Time

Influence of time on the efficiency of ZnCuBi-NO_3/SO_4 LDH for degradation of MB was examined in the range of 5–30 min. In a typical procedure, 10 mL of 10 mg L^{-1} MB

of pH 8 was taken into a 25 mL bottle containing 10 mg of the LDH. The mixture was exposed in visible light of a 100 W Tungsten lamp and stirred for 5–30 min at 25°C. The mixture was centrifuged and subjected to UV/Visible spectrophotometer at λ_{max} of 664 nm for quantification. The degradation efficiency was increased 93.98%–96.39% with increasing of time in the range of 5–30 min as depicted in Fig. 11a and b. Therefore, 30 min was chosen as the optimum time for further experiments.

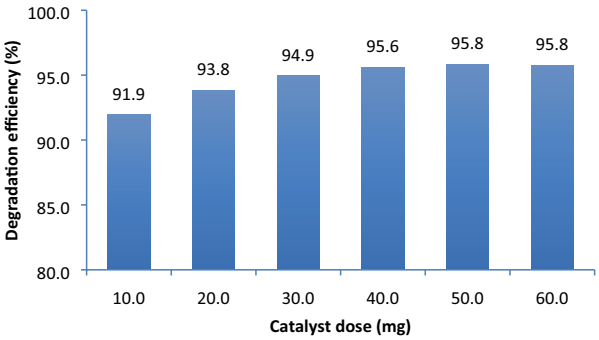

Fig. 10. Effect of LDH dosage on degradation efficiency (%) for MB.

4. Application of the method

The proposed method was applied to synthetic solutions. All the synthetic solutions of MB were prepared in tap water, wastewater, and seawater of different concentrations. The method worked well with a degradation efficiency of ≥89.70% with RSD ≤ 4.0% as shown in Table 3.

5. Comparison with other materials

Various LDHs materials have been reported for adsorptive and/or photocatalytic degradative removal of MB. The band gap energy of synthesized material ZnCuBi-NO_3/SO_4 LDH is 1.73 eV as shown in Table 4, which is comparatively lower and worked well as photocatalyst for the degradation of MB.

6. Conclusion

In this study, nanostructured ZnCuBi-NO_3/SO_4 LDH was synthesized by co-precipitation method from precursor salts of $ZnSO_4{\cdot}7H_2O$, $CuSO_4{\cdot}5H_2O$, and $Bi(NO_3)_3{\cdot}5H_2O$, and well characterized by FT-IR, XRD, EDX-SEM, and TGA. Using absorbance data, Tauc plot was plotted and band gap energy of ZnCuBi-NO_3/SO_4 LDH was calculated and found to be 1.73 eV. Thereafter, photocatalysis

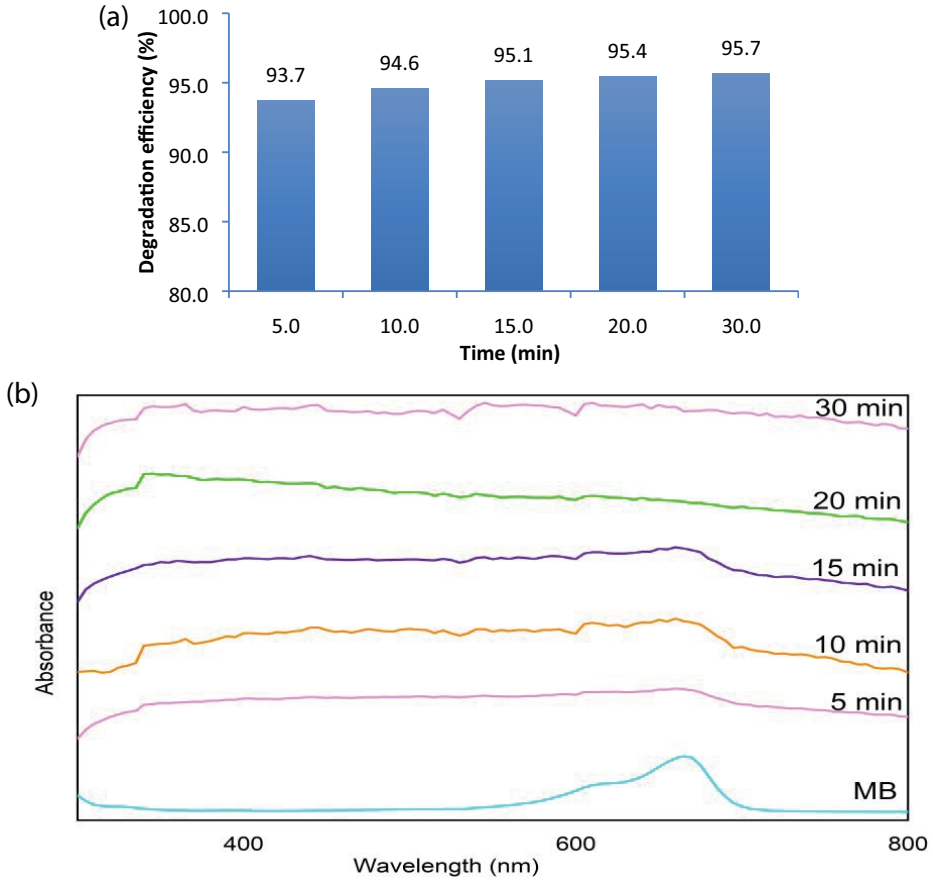

Fig. 11. (a) Effect of time on degradation efficiency (%) of LDH for MB. (b) UV-Visible spectra of degraded solutions of MB at different time.

was triggered by exposing the mixture under the visible light of a 100 W Tungsten lamp and stirring at 25°C for 30 min. Mechanistically, degradation was initiated when highly reactive hydroxyl radicals were generated and degradation of MB was triggered and degraded to the least harmful fragments. The degradation efficiency of the LDH was calculated and found to be ≥95.50% with RSD ≤4.0%. The method worked well on the synthetic solutions of MB, prepared in tap water, wastewater, and seawater of different concentrations. This study offers to develop economical and efficient LDH based photocatalyst for the treatment of MB contaminanted water at laboratory and industrial levels.

Table 3
Degradation of MB in synthetic solution

Samples	Concentration (mg L^{-1})	Degradation efficiency (%) ± RDS (%)
S-I	05	98.70 ± 2.1
	10	95.08 ± 3.3
	15	93.73 ± 2.2
	20	89.80 ± 2.5
S-II	05	98.4 ± 3.7
	10	96.5 ± 2.1
	15	93.1 ± 3.2
	20	89.7 ± 4.0
S-III	05	97.4 ± 3.2
	10	95.7 ± 2.5
	15	92.1 ± 3.0
	20	90.8 ± 3.5

S-I: Synthetic solution prepared in tap water in the Research Laboratory, Institute of Chemistry, University of Sindh, Jamshoro, Pakistan.
S-II: Synthetic solution prepared in wastewater, collected from the Industrial Area in Kotri, Pakistan.
S-III: Synthetic solution prepared in seawater, collected from the Sea in Karachi, Pakistan.

Acknowledgment

The authors gratefully acknowledge financial support from the Higher Education Commission, Islamabad, Pakistan. Project granted under NRPU Program (No. NRPU-8100).

References

[1] J.W. Moore, Inorganic Contaminants of Surface Water: Research and Monitoring Priorities, Springer, New York, 2012.
[2] G.M. Gadd, Metals, minerals and microbes: geomicrobiology and bioremediation, Microbiology, 156 (2010) 609–643.
[3] M. Halim, P. Conte, A. Piccolo, Potential availability of heavy metals to phytoextraction from contaminated soils induced by exogenous humic substances, Chemosphere, 52 (2003) 265–275.
[4] R.A.K. Rao, M. Kashifuddin, Kinetics and isotherm studies of Cd(II) adsorption from aqueous solution utilizing seeds of bottlebrush plant (*Callistemon chisholmii*), Appl. Water Sci., 4 (2014) 371–383.
[5] M. Husain, Q. Husain, Applications of redox mediators in the treatment of organic pollutants by using oxidoreductive enzymes: a review, Crit. Rev. Env. Sci. Technol., 38 (2007) 1–42.
[6] I. Michael, L. Rizzo, C.S. McArdell, C.M. Manaia, C. Merlin, T. Schwartz, C. Dagot, D. Fatta-Kassinos, Urban wastewater treatment plants as hotspots for the release of antibiotics in the environment: a review, Water Res., 47 (2013) 957–995.
[7] L.C. Davies, C.C. Carias, J.M. Novais, S. Martins-Dias, Phytoremediation of textile effluents containing azo dye by using *Phragmites australis* in a vertical flow intermittent feeding constructed wetland, Ecol. Eng., 25 (2005) 594–605.
[8] A. Ejraei, M.A. Aroon, A.Z. Saravani, Wastewater treatment using a hybrid system combining adsorption, photocatalytic degradation and membrane filtration processes, J. Water Process Eng., 28 (2019) 45–53.
[9] G. Sanjeev, A. Harshita, T. Manisha, A. Ali, S. Hemam, K. Rajwant, A. Mojtaba, Metal oxides and metal organic frameworks for the photocatalytic degradation: a review, J. Environ. Chem. Eng., 8 (2020) 103726, doi: 10.1016/j.jece.2020.103726.
[10] E.A.S. Dimapilis, C.S. Hsu, R.M.O. Mendoza M.C. Lu, Zinc oxide nanoparticles for water disinfection, Sustainable Environ. Res., 28 (2018) 47–56.

Table 4
Different LDHs for degradation of MB

LDHs	BE (eV)	pH	MB (mg L^{-1})	D/R (%)	Time (min)	References
ZnTi	3.06	–	5.0	100.0	10	[37]
ZnAlTi	3.08	7.0	10.0	99.0	30.0	[38]
CoCr	2.48	–	100.0	92.0	180.0	[39]
MgAl	–	6.8	10.0	31.9	60.0	[40]
NiTi	2.68	11.0	0.3	99.8	15.0	[41]
ZnCrBi	–	–	2.0	99.0	120.0	[42]
ZnCr	–	–	2.0	63.0	120.0	[42]
ZnAl	–	–	6.4	26.0	60.0	[43]
$NiFeTi_2$	–	4–12	20.0	96.8	1.0	[44]
ZnFe	–	6.0	10.0	57.0	30.0	[45]
MgFe	–	6.0	10.0	81.0	30.0	[45]
MnFe	–	6.0	10.0	70.0	30.0	[45]
ZnCuBi	1.73	8.0	10.0	95.5	30.0	This work

BE: Band gap energy; MB: Methylene blue; D/R (%): Degradation/Removal efficiency

[11] D. Wang, X. Li, J. Chen, X. Tao, Enhanced photoelectrocatalytic activity of reduced graphene oxide/TiO_2 composite films for dye degradation, Chem. Eng. J., 198–199 (2012) 547–554.
[12] J.G. Mahy, R.G. Tilkin, S. Douven, S.D. Lambert, TiO_2 nanocrystallites photocatalysts modified with metallic species: comparison between Cu and Pt doping, Surf. Interfaces, 17 (2019) 100366, doi: 10.1016/j.surfin.2019.100366.
[13] N. Yusoff, N.M. Huang, M.R. Muhamad, S.V. Kumar, H.N. Lim, I. Harrison, Hydrothermal synthesis of CuO/functionalized graphene nanocomposites for dye degradation, Mater. Lett., 93 (2013) 393–396.
[14] J. Ahmad, K. Majid, Enhanced visible light driven photocatalytic activity of CdO–graphene oxide heterostructures for the degradation of organic pollutants, New J. Chem., 42 (2018) 3246–3259.
[15] H. Seema, K. Christian Kemp, V. Chandra, K.S. Kim, Graphene-SnO_2 composites for highly efficient photocatalytic degradation of methylene blue under sunlight, Nanotechnology, 23 (2012) 355705, doi: 10.1088/0957-4484/23/35/355705.
[16] B. Chai, J. Li, Q. Xu, K. Dai, Facile synthesis of reduced graphene oxide/WO_3 nanoplates composites with enhanced photocatalytic activity, Mater. Lett., 120 (2014) 177–181.
[17] X. Chen, J. Dai, G. Shi, L. Li, G. Wang, H. Yang, Visible light photocatalytic degradation of dyes by β-Bi_2O_3/graphene nanocomposites, J. Alloys Compd., 649 (2015) 872–877.
[18] L. Jiade, W. Longfu, Y. Changlin, F. Wen, X. Yu, Z. Wanqin, Z. Lihua, Preparation and characterization of graphene oxide/Ag_2CO_3 photocatalyst and its visible light photocatalytic activity, Appl. Surf. Sci., 358 (2015) 168–174.
[19] M.A. Kausor, A.M. Ali, S.S. Gupta, D. Chakrabortty, Synthesis, characterization, and application of graphene-based silver orthophosphate nanocomposite in organic dye degradation, Desal. Water Treat., 140 (2019) 337–346.
[20] K. Morimoto, K. Tamura, N. Iyi, J. Ye, H. Yamada, Adsorption and photodegradation properties of anionic dyes by layered double hydroxides, J. Phys. Chem. Solids, 72 (2011) 1037–1045.
[21] P. Cai, S. Ci, N. Wu, Y. Hong, Z. Wen, Layered structured CoAl/CdS-LDHs nanocomposites as visible light photocatalyst, Physica Status Solidi (a), 214 (2017) 1600910, doi: 10.1002/pssa.201600910.
[22] B. Bridier, M.A.G. Hevia, N. López, J. Pérez-Ramírez, Permanent alkene selectivity 55 enhancement in copper-catalyzed propyne hydrogenation by temporary CO supply, J. Catal., 278 (2011) 167–172.
[23] L. Ju, P. Wu, X. Lai, S. Yang, B. Gong, M. Chen, N. Zhu, Synthesis and characterization of fullerene modified ZnAlTi-LDO in the photo-degradation of bisphenol A under simulated visible light irradiation, Environ. Pollut., 228 (2017) 234–244.
[24] C.M. Puscasu, E.M. Seftel, M. Mertens, P. Cool, G. Carja, ZnTi-LDH and the derived mixed oxides as mesoporous nanoarchitectonics with photocatalytic capabilities, J. Inorg. Organomet. Polym., 25 (2015) 259–266.
[25] Y. Meng, S.J. Xia, J.L. Xue, S.L. Ni, Z.M. Ni, Synthesis, and photocatalytic degradation performance for rhodamine B of Zn-Cr-Cu composite metal oxides derived from layered double hydroxides, Chin. J. Inorg. Chem., 34 (2018) 1632.
[26] A. Elhalil, R. Elmoubarki, M. Farnane, A. Machrouhi, M. Sadiq, F.Z. Mahjoubi, S. Qourzal, N. Barka, Photocatalytic degradation of caffeine as a model pharmaceutical pollutant on Mg doped ZnO-Al_2O_3 heterostructure, Environ. Nanotechnol. Monit. Manage., 10 (2018) 63–72.
[27] D.Y. Wang, F.R. Costa, A. Vyalikh, A. Leuteritz, U. Scheler, D. Jehnichen, U. Wagenknecht, L. Häussler, G. Heinrich, One-step synthesis of organic LDH and its comparison with regeneration and anion exchange method, Chem. Mater., 21 (2009) 4490–4497.
[28] A. Elhalil, R. Elmoubarki, M. Farnane, A. Machrouhi, F.Z. Mahjoubi, M. Sadiq, S. Qourzal, M. Abdennouri, N. Barka, Novel Ag-ZnO-$La_2O_2CO_3$ photocatalysts derived from the layered double hydroxide structure with excellent photocatalytic performance for the degradation of pharmaceutical compounds, J. Sci.: Adv. Mater. Devices, 4 (2019) 34–46.
[29] D.G. Evans, X. Duan, Preparation of layered double hydroxides and their applications as additives in polymers, as precursors to magnetic materials and in biology and medicine, Chem. Commun., 5 (2006) 485–496.
[30] W. Li, A. Liu, H. Tian, D. Wang, Controlled release of nitrate and molybdate intercalated in Zn-Al-layered double hydroxide nanocontainers towards marine anticorrosion applications, Colloid Interface Sci. Commun., 24 (2018) 18–23.
[31] D.A. Islam, K. Barman, S. Jasimuddin, H. Acharya, Synthesis of ultrasmall and monodisperse sulfur nanoparticles intercalated CoAl layered double hydroxide and their electrocatalytic water oxidation reaction at neutral pH, Nanoscale, 11 (2019) 7560–7566.
[32] B.A. Baig, A. Elçi, A.N. Siyal, S. Dehrajd, Q.K. Panhwar, A. Ahmed, A.R. Bhattia, F. Ali, M.Y. Khuhawar, Facile synthesis and characterization of β-$Cd(OH)_2$ nanostructures for adsorptive removal of Cr(VI) ions from wastewater: a statistical approach for multivariate sorption optimization, Desal. Water Treat., 218 (2021) 270–280.
[33] J.T. Kloprogge, D. Wharton, L. Hickey, R.L. Frost, Infrared and Raman study of interlayer anions CO_3^{2-}, NO_3^-, SO_4^{2-} and ClO_4^- in Mg/Alhydrotalcite, Am. Mineral., 87 (2002) 623–629.
[34] J. Yang, C. Yu, X. Fan, Z. Ling, J. Qiu, Y. Gogotsi, Facile fabrication of MWCNT-doped NiCoAl-layered double hydroxide nanosheets with enhanced electrochemical performances, J. Mater. Chem. A, 1 (2013) 1963–1968.
[35] F.Z. Mahjoubi, A. Khalidi, M. Abdennouri, N. Barka, Zn–Al layered double hydroxides intercalated with carbonate, nitrate, chloride, and sulfate ions: synthesis, characterization and dye removal properties, J. Taibah Univ. Sci., 11 (2017) 90–100.
[36] X. Tao, K. Zheng, L. Huang, Plasma induced liquid-phase synthesis of Ce/Mo metal oxides as photocatalysts, Chem. Phys. Lett., 780 (2021) 138903, doi: 10.1016/j.cplett.2021.138903.
[37] M. Shao, J. Han, M. Wei, D.G. Evans, X. Duan, the synthesis of hierarchical Zn–Ti layered double hydroxide for efficient visible-light photocatalysis, Chem. Eng. J., 168 (2011) 519–524.
[38] W. Xiaorong. W. Pingxiao, H. Zhujian, Z. Nengwu, W. Jinhua, L. Ping, D. Zhi, Solar photocatalytic degradation of methylene blue by mixed metal oxide catalysts derived from ZnAlTi layered double hydroxides, Appl. Clay Sci., 95 (2014) 95–103.
[39] N. Baliarsingh, K.M. Parida, G.C. Pradhan, Effects of Co, Ni, Cu and Zn on photophysical and photocatalytic properties of carbonate intercalated M^{II}/Cr LDHs for enhanced photodegradation of methyl orange, Ind. Eng. Chem. Res., 53 (2014) 3834–3841.
[40] Y. Zhou, W. Hu, J. Yu, F. Jiao, Effective photocatalytic degradation of methylene blue by Cu_2O/MgAl layered double hydroxides, React. Kinet. Mech. Catal., 115 (2015) 581–596.
[41] P. Roy Chowdhury, K.G. Bhattacharyya, Retracted article: Ni/Ti layered double hydroxide: synthesis, characterization, and application as a photocatalyst for visible light degradation of aqueous methylene blue, Dalton Trans., 44 (2015) 6809–6824.
[42] M. Dinari, M.M. Momeni, Z. Bozorgmehr, S. Karimi, Bismuth-containing layered double hydroxide as a novel efficient photocatalyst for degradation of methylene blue under visible light, J. Iran. Chem. Soc., 14 (2017) 695–701.
[43] G. Starukh, Photocatalytically enhanced cationic dye removal with Zn-Al layered double hydroxides, Nanoscale Res. Lett., 12 (2017) 391, doi: 10.1186/s11671-017-2173-y.
[44] G. Rathee, A. Awasthi, D. Sood, R. Tomar, V. Tomar, R. Chandra, A new biocompatible ternary layered double hydroxide adsorbent for ultrafast removal of anionic organic dyes, Sci. Rep., 9 (2019) 16225, doi: 10.1038/s41598-019-52849-4.
[45] Z. Shi, Y. Wang, S. Sun, C. Zhang, H. Wang, Removal of methylene blue from aqueous solution using Mg-Fe, Zn-Fe, Mn-Fe layered double hydroxide, Water Sci. Technol., 81 (2020) 2522–2532.